High energy-resolution measurement of the ^{82}Se(^{3}He ,t)^{82}Br reaction for double-β decay and for solar neutrinos

D. Frekers,[1] M. Alanssari,[1,2] T. Adachi,[3] B. T. Cleveland,[4,*] M. Dozono,[5] H. Ejiri,[6,7] S. R. Elliott,[8] H. Fujita,[6,9] Y. Fujita,[9] M. Fujiwara,[6] K. Hatanaka,[6] M. Holl,[1] D. Ishikawa,[6] H. Matsubara,[10] H. Okamura,[6,†] P. Puppe,[1] K. Suda,[5] A. Tamii,[6] J. Thies,[1] and H. P. Yoshida[11]

[1]*Institut für Kernphysik, Westfälische Wilhelms-Universität Münster, D-48149 Münster, Germany*
[2]*Al-Nahrain University, Baghdad, Iraq*
[3]*Research Center for Electron and Photon Science, Tohoku University, Sendai, Miyagi 982-0826, Japan*
[4]*Department of Physics, University of Washington, Seattle Washington 98195, USA*
[5]*RIKEN, 2-1, Hirosawa, Wako, Saitama 351-0198, Japan*
[6]*Research Center for Nuclear Physics, Osaka University, Ibaraki, Osaka 567-0047, Japan*
[7]*Nuclear Physics, Czech Technical University, Prague, Czech Republic*
[8]*Los Alamos National Laboratory, Los Alamos, New Mexico 87545, USA*
[9]*Department of Physics, Osaka University, Toyonaka, Osaka 560-0043, Japan*
[10]*Center for Nuclear Study, University of Tokyo, 7-3-1 Hongo, Bunkyo, Tokyo 113-0033, Japan*
[11]*CYRIC, Tohoku University, Aramaki, Aoba, Sendai 980-8578, Japan*

(Received 23 May 2016; published 21 July 2016)

A high-resolution (^{3}He ,t) charge-exchange experiment at an incident energy of 420 MeV has been performed on the double beta ($\beta\beta$) decay nucleus ^{82}Se. A detailed Gamow-Teller (GT^{-}) strength distribution in ^{82}Br has been extracted, which provides information to the $\beta\beta$-decay nuclear matrix elements. Three strong and isolated transitions, which are to the 75, 1484 and the 2087 keV states in ^{82}Br, are found to dominate the low-excitation region below $\approx$2.1 MeV. Above 2.1 MeV a sudden onset of a strong GT fragmentation is observed. The degree of fragmentation resembles a situation found in the neighboring $A = 76$ system (^{76}Ge), whereas the observed concentration of strength in the three low-lying states is reminiscent of the heavier neighbors ^{96}Zr and ^{100}Mo. The strong GT transition to the 75 keV (1^{+}) state makes ^{82}Se interesting for solar neutrino detection. The ^{82}Se(ν_e,e^{-})^{82}Br solar neutrino capture rate in a nonoscillation scenario is therefore evaluated to $668 \pm 12(\text{stat}) \pm 60(\text{sys})$ SNU, and some of the advantages of using selenium for solar neutrino studies are discussed.

DOI: 10.1103/PhysRevC.94.014614

I. INTRODUCTION

The isotope ^{82}Se features several properties, which make it attractive for experiments related to neutrino properties and neutrino physics. Foremost, ^{82}Se is one of the prime candidates for observing the $\beta\beta$ decay because of its comparatively high Q value of $Q_{\beta\beta} = 2998$ keV [1], which is topped only by ^{48}Ca, ^{150}Nd, ^{96}Zr, and ^{100}Mo. The $2\nu\beta\beta$ decay half-life has recently been measured directly [2] and a recommended value is given as $T_{1/2}^{2\nu\beta\beta} = [9.2 \pm 0.7] \times 10^{19}$ yr in Ref. [3]. The most stringent limit on the alternative, neutrinoless decay variant is reported in Ref. [4] at $T_{1/2}^{0\nu\beta\beta} > 3.6 \times 10^{23}$ yr (90% C.L.), and in order to increase this limit in the future, the natural isotopic abundance of 8.7% as well as the chemistry for isotopic enrichment of ^{82}Se constitute favorable preconditions [5,6]. Furthermore, ^{82}Se may also be procured as a material for the detection of solar neutrinos, in particular of those originating from the pp reaction. Its potential is due the low Q value of $\approx$172 keV for the ^{82}Se(ν_e,e^{-})^{82}Br*(75keV,1^{+}) capture reaction (cf. Fig. 1). This is to be compared with 233 keV for ^{71}Ga, which was used in the SAGE and GALLEX experiments [7–11], and with 168 keV for ^{100}Mo in the MOON experiment [12]. Moreover, the transition to the 75 keV state carries a favorably large transition strength of $B(\text{GT}) = 0.34$. This value was extracted from a (p,n) experiment performed at 134.4 MeV at the Indiana University Cyclotron Facility [13] and is confirmed in the present experiment. However, a full response to the solar neutrinos warrants a GT distribution with high resolution, which will be presented in this article.

We also remark that $\beta\beta$-decaying nuclei have been receiving attention in the geological context. A recent geochemically determined $\beta\beta$-decay half-life of ^{82}Se was reported by Lin *et al.* [14] to $T_{1/2}(^{82}\text{Se}) = [12 \pm 1(\text{stat}) \pm 3.6(\text{sys})] \times 10^{19}$ yr along with a new half-life value for ^{130}Te at $T_{1/2}(^{130}\text{Te}) = [7.5 \pm 0.3(\text{stat}) \pm 2.3(\text{sys})] \times 10^{20}$ yr. (The 30% systematic errors quoted here were conjectured as realistic in Ref. [14].) Lin *et al.* used Kitkaite minerals (NiTeSe) from Northern Finland, which contained about similar amounts of selenium (30%) and tellurium (47%). This constitutes an advantage, since retention times for the two noble gas daughters ^{82}Kr and ^{130}Xe in the host lattice, though model dependent, are expected to be similar.

The above quoted, geochemically determined $\beta\beta$-decay half-lives are in remarkably good agreement with the most recently recommended values [3] for ^{82}Se and ^{130}Te from direct counting, i.e., $T_{1/2}^{2\nu\beta\beta}(^{82}\text{Se}) = [9.2 \pm 0.7] \times 10^{19}$yr and

[*] Also at SNOLAB, Lively, Ontario, Canada.
[†] Deceased.

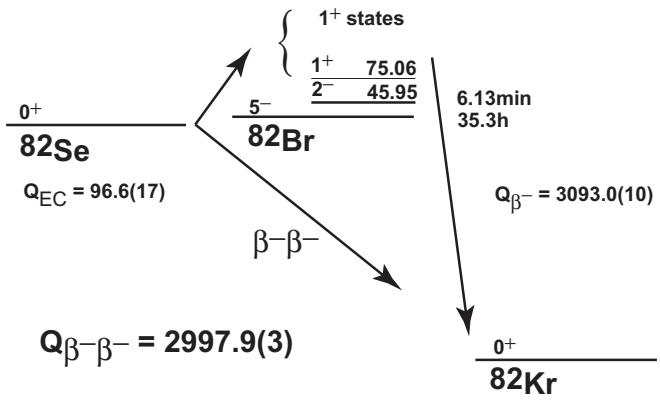

FIG. 1. Sketch of the $2\nu\beta\beta$ decay process in ^{82}Se. The transition paths through the intermediate 1^+ states in ^{82}Br are indicated. The various Q values and excitation energies are taken from Refs. [1,30,31]. All energies are given in keV units.

$T_{1/2}^{2\nu\beta\beta}(^{130}\text{Te}) = [6.9 \pm 1.3] \times 10^{20}$yr. Nonetheless, the modeling of the time of mineralization, as well as of the retention times for the noble gases, and the assumptions made about alternative productions through fission, fission induced neutrons or cosmic rays over geological time scales, remain the main sources of systematic uncertainties in geochemical analyses. On the other hand, by today's good knowledge of many $2\nu\beta\beta$-decay half-lives one is now in the position to constrain many of these assumptions. This is indicated in detail in Ref. [14].

In this article the ^{82}Se(^{3}He,t)^{82}Br reaction has been used to provide a detailed and high-resolution insight into the GT strength distribution in ^{82}Br, as this ties in to some of the aforementioned subjects. One may recall that hadronic charge-exchange reactions at intermediate energies (i.e., 100–300 MeV/A) and low momentum transfers $q_{tr} \approx 0$ fm^{-1} are a well-established tool to selectively induce GT transitions [15]. This follows from the dominant $\sigma\tau$ component of the effective nucleon-nucleon (NN) interaction in this energy/momentum region [16–20], where, in addition, the nucleus exhibits a high nuclear transparency.

The present experiment is within the spirit of previous high-resolution (^{3}He,t) charge-exchange experiment on light and medium-weight nuclei reported in Refs. [15,21–28], and many details of the reactions and analyses can be found there. Charge-exchange reactions for $\beta\beta$ decay and astrophysical neutrino studies are, for instance, reviewed in Ref. [29].

II. EXPERIMENT

The experiment was performed at Research Center for Nuclear Physics (RCNP), Osaka University. A 420 MeV ^{3}He^{++} beam was accelerated using the Azimuthally Varying Field (AVF) Cyclotron in combination with the Ring Cyclotron and transported to the scattering chamber of the Grand Raiden Spectrometer [32]. The West-South (WS) beam line [33] provided the dispersion of the beam necessary for obtaining high-resolution (^{3}He,t) spectra. Several tuning techniques for dispersion matching between beam line and spectrometer were employed to optimize energy and angular resolution. These are described in Refs. [32–36].

Outgoing reaction tritons were momentum analyzed in the Grand Raiden Spectrometer within its full acceptance of ±20 mrad in horizontal and ±40 mrad in vertical direction. The detection system consisted of a set of two mutliwire drift chambers, which allowed precise track reconstruction on the focal plane [37]. They were followed by two thin (3 and 10 mm) plastic scintillators used for particle identification and for providing the event trigger.

A thin 1.79(5) mg/cm^2 Se target evaporated on a 150 μg carbon backing was employed. The target thickness was determined by performing an energy-loss measurement of α particles traversing the target foil in a specially designed setup. The thickness calculation was done with the computer code SRIM [38]. The Se material was isotopically enriched and specified at 97.43(2)% ^{82}Se.

After applying various off-line spectrometer aberration corrections, a final-state energy resolution of 38 keV was obtained, which was partly due to the energy-loss differences between ^{3}He and triton ions in the target.

An energy calibration was performed using a ^{26}Mg and a $^{\text{nat}}$Si target. These targets provide numerous levels at well-known excitation energies distributed over a large momentum in the focal plane. In the energy region up to the isobaric analog state (IAS) the accuracy is at a level of ±2keV. Two spectrometer-angle settings, i.e., 0° and 2.5°, allowed generating center-of-mass (c.m.) angular distributions ranging from $\theta_{\text{c.m.}} \approx 0°$ to $\theta_{\text{c.m.}} \approx 4.0°$.

III. ANALYSIS

Excitation-energy spectra of the ^{82}Se(^{3}He,t)^{82}Br reaction are shown in Fig. 2. Three angular cuts have been overlaid to visualize the behavior of the angular distribution.

The spectra are dominated by the strongly excited IAS, which is located at an excitation energy of $E_x = 9.576$ MeV. This energy agrees well with the value of $E_x = 9.58$ MeV reported in Ref. [13] from a ^{82}Se(p,n) reaction at 134.4 MeV and with an energy resolution of about 300 keV. The broad Gamow-Teller resonance (GTR) appears above the IAS at an excitation energy of $E_x \approx 12.1$ MeV and has a width of ≈5 MeV.

The low excitation energy region is dominated by a GT transition to the 75 keV (1^+) state. The lowest excited state at 45.9 keV (2^-) (cf. Fig. 1) was too weakly populated at these angles to be identified against the strong 1^+ state at 75 keV.

It appears that the spectra below ≈2.1 MeV excitation energy show a remarkably low level of fragmentation, contrary, for instance, to its close-by neighbor ^{76}Ge [22]. Only three strongly excited $J^\pi = 1^+$ states, at 75, 1484, and 2087 keV appear in the spectra. On the other hand, the fragmentation suddenly increases dramatically above ≈2.1 MeV. In total, more than 60 states below 6 MeV were identified above a general background dominated by the tail of the GTR. This situation is more reminiscent of the ^{76}Ge case shown in Ref. [22], where this high level of fragmentation was attributed to the softness of the nuclear shape near $A = 76$.

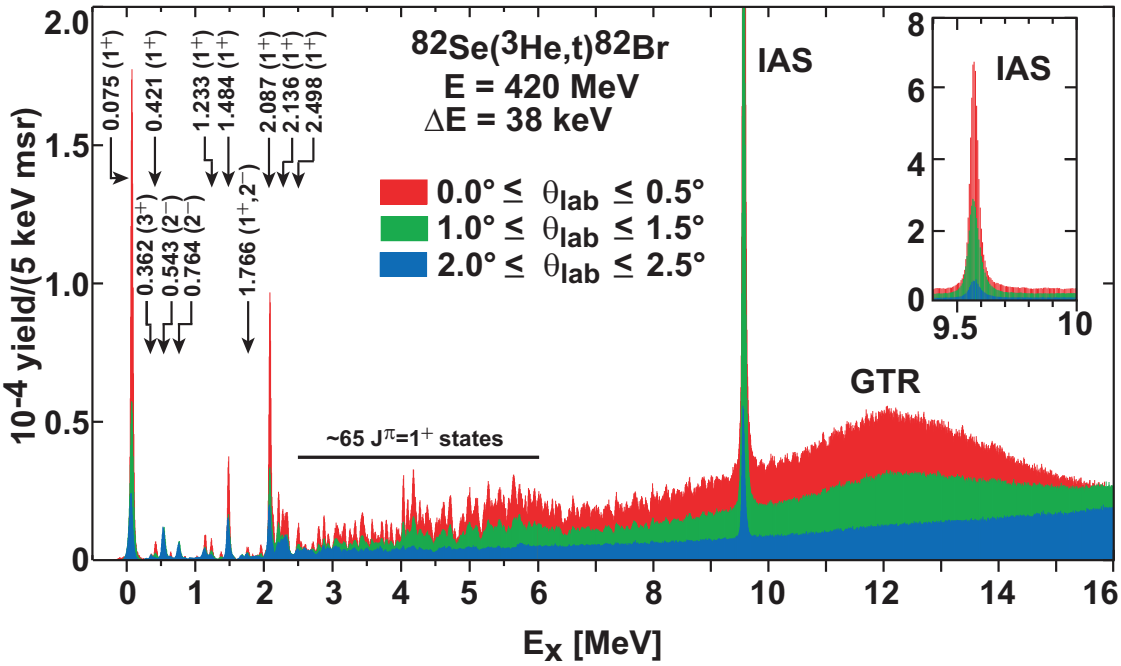

FIG. 2. Excitation-energy spectra of the ^{82}Se(^{3}He ,t)^{82}Br reaction. The spectra were generated from three different angle cuts (indicated by colors) and overlaid to show the effect of the angular dependence. $\Delta L = 0$ transitions (GT and IAS) are forward-peaked and prominently appear in the spectrum at $0.0^\circ \leqslant \theta_{\rm lab} \leqslant 0.5^\circ$. Note, the energy scale is modified above 6 MeV. The inset magnifies the IAS region.

A. Distorted wave calculations

The angular distributions are shown in Fig. 3 for different isolated transitions. Distorted-wave (DW) calculations were performed to describe the cross-section angular distributions. They were performed in the same way as, for instance, described in Refs. [15,22] using the code FOLD [39] and the Love-Franey nucleon-nucleon interactions [18].

Optical-model parameters were interpolated from Ref. [40] for the case of a ^{82}Se target and a ^{3}He projectile. In the outgoing channel the triton potential depths were reduced by 15% according to the prescription in Ref. [41]. The relevant optical-model parameters are given in Table I. Single-particle wave functions were generated in a Woods-Saxon potential with a radius of $r_0 = 1.25$ fm, and transition amplitudes were derived from the code NORMOD [42].

Transitions to $J^\pi = 1^+$ final states in ^{82}Br can be mediated by $\Delta L = 0$ and $\Delta L = 2$ transition amplitudes. Both amplitudes are necessary to describe the experimental angular distributions over the full angular range. The different ΔL components should be added coherently to the cross section, however, due to the lack of a realistic underlying nuclear model, one is simply left to add them in an incoherent way. We note that for $J^\pi = 1^+$ transitions there seems to be a tendency of increasing $\Delta L = 2$ contributions with increased target mass. This has been observed for ^{96}Zr, ^{100}Mo, ^{128}Te, ^{130}Te, and ^{136}Xe [23–26] and attributed to an increasing number of matching open orbits near the Fermi surface [23], as $(N - Z)$ increases from $(N - Z) = 14$ (^{82}Se) to $(N - Z) = 28$ (^{136}Xe).

TABLE I. Optical model parameters used for the ^{82}Se(^{3}He ,t) reaction calculations.

projectile ejectile	V_R [MeV]	r_R [fm]	a_R [fm]	W_I [MeV]	r_I [fm]	a_I [fm]
^{3}He	−36.67	1.33	0.825	−52.0	0.991	1.056
^{3}H	−31.17	1.33	0.825	−44.2	0.991	1.056

B. Determination of Gamow-Teller strength

The key relation for extracting the GT strength from the (^{3}He ,t) charge-exchange reaction cross sections extrapolated to $q = 0$ is given by

$$\left.\frac{d\sigma^{\rm GT}}{d\Omega}\right|_{q=0} = \left(\frac{\mu}{\pi\hbar^2}\right)^2 \frac{k_f}{k_i} N_D^{\sigma\tau} |J_{\sigma\tau}|^2 B({\rm GT}), \qquad (1)$$

where $J_{\sigma\tau}$ is the volume integral of the effective interaction, $N_D^{\sigma\tau}$ the optical-model distortion factor, and k_i and k_f are the initial and final momenta. At a reasonably high level of accuracy (≈3%), the value for the volume integral of the effective interaction is $J_{\sigma\tau} = 161.5$ MeV fm^3 [15,18]. The distortion factor $N_D^{\sigma\tau}$ can be evaluated from the ratio between the plane-wave and distorted-wave cross section at $q = 0$ (but see also Ref. [15]), i.e.,

$$N_D^{\sigma\tau} = \frac{\sigma_{DW}(q=0)}{\sigma_{PW}(q=0)} \qquad (2)$$

which leads to $N_D^{\sigma\tau} = 0.0559$ in the case of ^{82}Se. This value is within 1% of the value calculated by an eikonal approach [15,43], i.e.,

$$N_D^{\sigma\tau} = \exp(1\text{–}0.895A^{1/3}). \qquad (3)$$

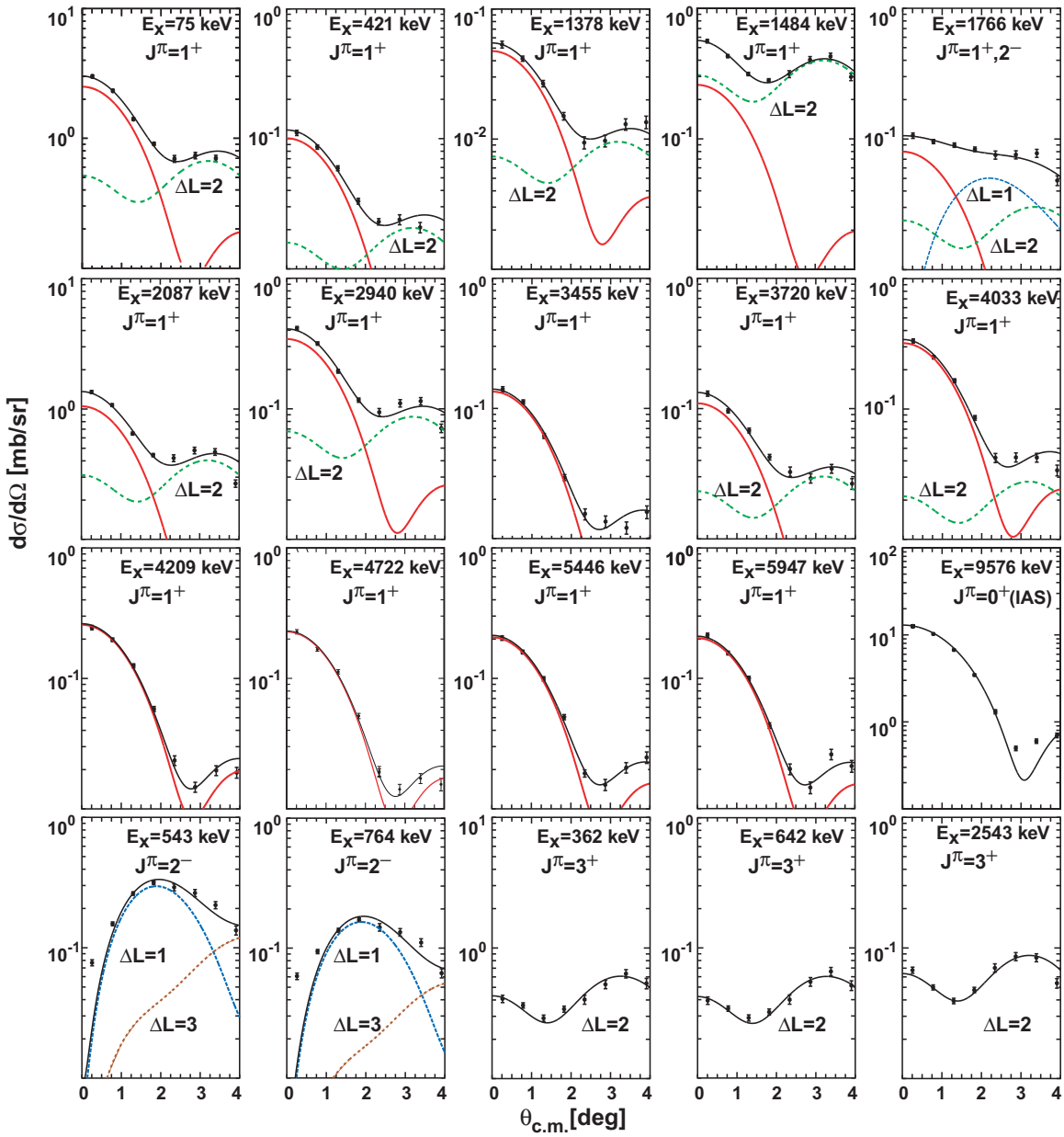

FIG. 3. Selected angular distributions for the ^{82}Se(^{3}He,t)^{82}Br reaction (sorted by $J^\pi = 1^+,0^+,2^-,3^+$ final state excitations).

By using Eq. (1) the extraction of the B(GT) strength is straightforward. The $q = 0$ extrapolation can be performed via a zeroth-order Bessel function, $|j_0(q\ R)|^2$, with R being the nuclear radius typically set to $1.25A^{1/3}$. Table II lists all relevant data extracted for the single states up to 6 MeV excitation. In the case of a multipole decomposition of the cross sections, the errors of the extracted B(GT) values include an arbitrary 50% contribution from the non-GT part of the cross section at $q = 0$ on top of the statistical errors. We consider this the most conservative approach to account for the lack of the coherent summation of the $\Delta L = 0$ and $\Delta L = 2$ amplitudes at $q = 0$.

In a similar way an analysis of the IAS at 9.576 MeV was performed by using $J_\tau = 63(2)$ MeV fm^3 for the volume integral of the effective interaction and by following the prescription of the $q = 0$ extrapolation given in Ref. [15]. The calculated Fermi strength then comes to $B(F) = 13.8 \pm 0.5$ in accordance with the expected value $(N - Z) = 14$.

The integrated B(GT) strength from the analysis of the individual states up to 6 MeV excitation yields $\sum B(\mathrm{GT}) = 1.98 \pm 0.04(\mathrm{stat})$. A consistency check was made by analyzing in the same way the angular-distribution cross sections integrated over 0.5 MeV energy bins. The results are shown in Fig. 4. The extracted B(GT) values are listed in Table III and compared with the values extracted from individual states. As expected, with the onset of fragmentation above 2 MeV, the procedure of extracting the B(GT) strength from individual states fails to account for the underlying contribution from the rather structureless tail of the GTR. This is also indicated in Fig. 5 for the individual states and in Fig. 6 for the running sums.

TABLE II. Excitation energies, cross sections, B(GT) values for low-lying states populated through the ^{82}Se(^{3}He,t)^{82}Br reaction (two tables, left and right). In column one, excitation energies from Ref. [31] (spins quoted if known, errors if significant) are compared with those from the (^{3}He,t) reaction in column three (errors ±2 keV) (not in right table), followed by cross sections at $q = 0$, their GT fraction and the extracted B(GT) values. Cross-section errors are statistical ones only. Errors for B(GT) values include an extra 50% contribution from the non-GT part of the cross section at $q = 0$. Spin assignments in square brackets indicate the presence of closely spaced and unresolved states with different spins. Dividing lines are between full MeV values.

^{82}Br (Ref. [31])		^{82}Br		$\frac{d\sigma}{d\Omega}(q=0)$	GT	B(GT)	^{82}Br		$\frac{d\sigma}{d\Omega}(q=0)$	GT	B(GT)
E_x[keV]	J^π	E_x[keV]	J^π	[mb/sr]	%		E_x[keV]	J^π	[mb/sr]	%	
75.06	1^+	75	1^+	3.009(52)	82	0.338(31)	4033	1^+	0.35(7)	94	0.046(9)
362.80	(1^+)	362	3^+	–	–	–	4099	1^+	0.250(6)	91	0.032(2)
420.07	(2)	421	1^+	0.116(15)	86	0.014(2)	4170	1^+	0.373(8)	94	0.049(2)
540.99	$(2^+,3^+)$	543	2^-	–	–	–	4209	1^+	0.267(6)	98	0.037(1)
641.16	(3^+)	642	3^+	–	–	–	4272	1^+	0.230(5)	92	0.030(1)
763.71	$(1)^+$	764	2^-	–	–	–	4317	1^+	0.131(3)	99	0.018(1)
849.69	$(1^+,2,3^+)$	848	1^+	0.030(1)	14	0.0010(5)	4365	1^+	0.112(3)	94	0.015(1)
1139.93		1142	1^+	0.173(4)	28	0.007(3)	4391	1^+	0.120(3)	100	0.017(1)
1232.57(3)		1233	1^+	0.140(4)	68	0.013(2)	4433	1^+	0.110(3)	88	0.013(1)
1386(8)	$(^+)$	1378	1^+	0.055(1)	87	0.0070(4)	4511	1^+	0.086(3)	99	0.012(1)
(1489)		1484	1^+	0.567(9)	46	0.036(10)	4554	$[1^+,2^-]$	0.101(2)	96	0.014(1)
1678		1680	2^-	–	–	–	4601	1^+	0.141(4)	92	0.018(1)
(1774)		1766	$[1^+,2^-]$	0.106(2)	75	0.011(1)	4632	1^+	0.157(4)	88	0.019(1)
1955(4)		1958	1^+	0.100(2)	74	0.010(1)	4689	$[1^+,2^-]$	0.106(3)	93	0.014(1)
		2087	1^+	1.366(4)	77	0.149(17)	4772	1^+	0.243(6)	98	0.033(1)
		2136	1^+	0.258(6)	72	0.026(4)	4779	2^-	–	–	–
		2213	$[1^+,2^-]$	0.403(9)	90	0.051(3)	4869	1^+	0.088(2)	85	0.010(1)
		2272	1^+	0.315(9)	55	0.024(5)	4910	1^+	0.136(4)	93	0.018(1)
		2317	1^+	0.247(7)	21	0.007(3)	4971	1^+	0.206(5)	92	0.026(1)
		2351	1^+	0.227(4)	67	0.021(4)	5008	1^+	0.235(6)	97	0.032(1)
		2498	1^+	0.162(3)	73	0.017(2)	5066	1^+	0.176(4)	88	0.022(1)
		2543	3^+	–	–	–	5110	1^+	0.224(8)	98	0.031(1)
		2712	1^+	0.068(1)	58	0.006(1)	5211	1^+	0.129(3)	91	0.016(1)
		2801	1^+	0.154(3)	87	0.019(1)	5250	1^+	0.126(4)	100	0.017(1)
		2876	1^+	0.185(4)	72	0.019(3)	5279	1^+	0.244(6)	97	0.033(1)
		2940	1^+	0.412(7)	84	0.049(4)	5326	1^+	0.186(4)	94	0.024(1)
		3028	1^+	0.092(2)	74	0.010(1)	5371	1^+	0.189(5)	99	0.026(1)
		3062	1^+	0.126(3)	78	0.014(2)	5416	1^+	0.168(4)	95	0.022(1)
		3097	3^+	–	–	–	5446	1^+	0.219(5)	97	0.029(1)
		3172	1^+	0.137(3)	79	0.015(2)	5491	1^+	0.162(5)	100	0.023(1)
		3256	1^+	0.098(2)	82	0.011(1)	5519	1^+	0.086(3)	97	0.012(1)
		3296	1^+	0.046(1)	39	0.003(1)	5571	1^+	0.170(4)	95	0.023(1)
		3333	1^+	0.140(3)	81	0.016(2)	5614	1^+	0.124(5)	100	0.017(1)
		3420	1^+	0.167(4)	88	0.020(1)	5641	1^+	0.185(5)	100	0.026(1)
		3455	1^+	0.142(4)	96	0.019(1)	5671	1^+	0.222(7)	100	0.031(1)
		3507	3^+	–	–	–	5712	$[1^+,2^-]$	0.117(4)	99	0.016(1)
		3579	1^+	0.125(3)	90	0.016(1)	5727	1^+	0.143(4)	100	0.020(1)
		3623	1^+	0.066(2)	65	0.006(1)	5761	1^+	0.197(5)	98	0.027(1)
		3688	$[1^+,2^-]$	0.050(1)	55	0.004(1)	5810	$[1^+,2^-]$	0.153(4)	99	0.021(1)
		3720	1^+	0.135(3)	83	0.016(1)	5866	1^+	0.224(5)	93	0.029(1)
		3788	1^+	0.125(3)	91	0.016(1)	5908	1^+	0.124(3)	91	0.016(1)
		3856	1^+	0.095(2)	85	0.011(1)	5947	1^+	0.217(5)	97	0.029(1)
		3951	1^+	0.091(2)	67	0.009(2)					$\sum = 1.98(4)$

In the present analyses we have restricted ourselves to the low-excitation region. This has also been the objectives of previous works on (^{3}He,t) charge-exchange reactions [15,21–26]. In fact, it has been shown in those previous studies that, although the GTR is the most prominent feature in the spectra of (p,n)-type charge-exchange reactions carrying the bulk of the GT strength, it has little impact on the size of the $2\nu\beta\beta$-decay nuclear matrix elements. This is a consequence of the Pauli blocking, which prevents the GTR to couple to the ground state of the $\beta\beta$ decay daughter via a $\Delta L = 0$,

TABLE III. B(GT) values extracted from 0.5 MeV energy bins and compared with those of individual states summed over the same energy bin (up to 6 MeV). The integrated B(GT) strength extends to 7.6 MeV, which is the threshold for neutron emission. The errors on the integrated strengths are evaluated by adding in quadrature the individual errors.

^{82}Br E_x [MeV]	%GT	B(GT) $\Delta E = 0.5$ MeV	B(GT) indiv. states
0.0–0.5	81	0.352(33)	0.352(31)
0.5–1.0	79	0.025(5)	0.0010(5)
1.0–1.5	58	0.066(14)	0.063(11)
1.5–2.0	65	0.042(7)	0.022(2)
2.0–2.5	67	0.284(47)	0.295(19)
2.5–3.0	62	0.117(22)	0.093(5)
3.0–3.5	75	0.215(27)	0.109(4)
3.5–4.0	80	0.219(22)	0.078(3)
4.0–4.5	91	0.449(20)	0.258(10)
4.5–5.0	91	0.403(18)	0.168(3)
5.0–5.5	92	0.543(22)	0.279(3)
5.5–6.0	92	0.608(24)	0.269(3)
6.0–6.5	92	0.497(19)	–
6.5—7.0	93	0.498(17)	–
7.0–7.6	93	0.615(17)	–
		$\sum_{0\text{–}6\ \text{MeV}} = 3.32(9)$	$\sum_{0\text{–}6\ \text{MeV}} = 1.98(4)$
		$\sum_{0\text{–}7.6\ \text{MeV}} = 4.93(9)$	–

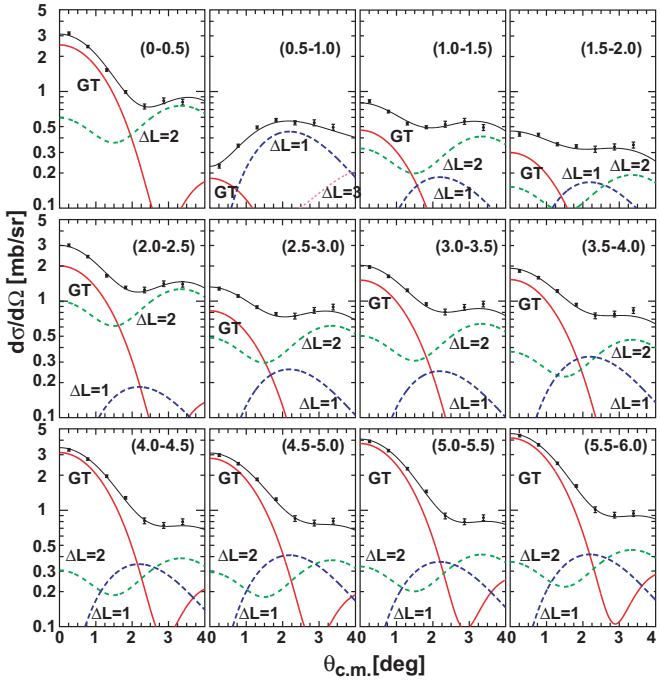

FIG. 4. Angular distributions of the ^{82}Se(^{3}He,t)^{82}Br reaction for the energy bins of $\Delta E = 500$ keV compared with DW model calculations. The various angular-momentum-transfer contributions are indicated. The $\theta = 0^\circ$ cross sections and the extracted GT strengths are given in the Tables II and III.

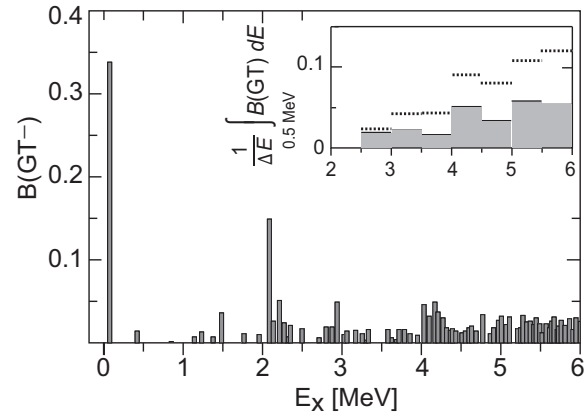

FIG. 5. B(GT) strength distribution for the ^{82}Se(^{3}He,t)^{82}Br reaction. The inset shows the average B(GT) strength per $\Delta E = 100$ keV for an energy bin of 500 keV. The dotted line shows the integration when taking the full spectrum, and the histograms show the sum over the individual states (cf. Table III). The figure indicates that above ≈2.5 MeV the contribution from the rather structureless GTR tail gets to be appreciable.

GT$^+$ transition, which is contrary to the low-lying states near the Fermi surface [29]. Possible phase cancellations in Eq. (5), which have been discussed in Ref. [44] may even further lower the significance of the GTR for $\beta\beta$ decay.

C. Implications for $\beta\beta$ decay

Since the details of the GT distribution at low excitation energies mirror the underlying nuclear structure, the present data provide relevant information for models aimed at calculating the $2\nu\beta\beta$- as well as the $0\nu\beta\beta$-decay nuclear matrix elements. In both cases the nuclear matrix elements represent the coupling between the transitions from mother to daughter via the intermediate nucleus. For the $2\nu\beta\beta$ case this coupling is particularly simple, because it only connects allowed GT$^-$ isospin-lowering $T_<$ transition amplitudes with allowed GT$^+$ isospin-raising $T_>$ ones [15]. Using the general notation (cf.

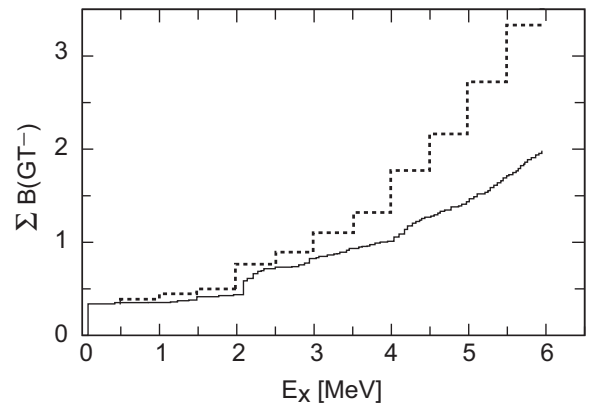

FIG. 6. Running sum of the B(GT) strength by integrating over individual states (full line) and over 500 keV energy bins (broken line).

Refs. [45] and [46], where only the $\sigma\tau$ and τ parts are retained and assuming the light Majorana ν-mass process), the two partial half-lives are given by

$$\left(T_{1/2}^{0\nu}\right)^{-1} = G^{0\nu}(Q,Z)g_A^4\left|M_{\sigma\tau}^{0\nu} - \frac{g_V^2}{g_A^2}M_{\tau}^{0\nu}\right|^2\left|m_{\nu_e}\right|^2,$$
$$\left(T_{1/2}^{2\nu}\right)^{-1} = G^{2\nu}(Q,Z)g_A^4\left|M_{GT}^{2\nu}\right|^2. \quad (4)$$

In the neutrinoless case the nuclear matrix elements are ordinary numbers, whereas in the 2ν case they carry an additional energy-weighting factor, which depends on the $\beta\beta$ decay Q value ($Q_{\beta\beta}$) and the energy difference between the intermediate 1^+ state and the initial ground state ($E_x(1_m^+) - E_0$):

$$M_{GT}^{2\nu} = \sum_m \frac{M_m(\mathrm{GT}^-)M_m(\mathrm{GT}^+)}{{}^1\!/_2 Q_{\beta\beta} + E_x(1_m^+) - E_0}. \quad (5)$$

The transition amplitudes are connected to the B(GT) values via (assuming a $0^+ \rightarrow 0^+$ decay)

$$|M(\mathrm{GT})|^2 = B(\mathrm{GT}) \quad (6)$$

In Ref. [22] it was conjectured that fragmentation and moreover, the lack of a correlation between the $B(\mathrm{GT}^-)$ and the $B(\mathrm{GT}^+)$ transitions of mother and daughter nucleus [Eq. (5)] are a result of their different deformations and/or their soft surfaces. This argument is well supported by numerous theoretical calculations [47–50]. In fact, these have shown that the size of the matrix elements for both decay variants is significantly reduced as a result of a shape difference between mother and daughter nucleus, and it was argued that experimental GT distributions can be important ingredients to advance the calculations of matrix elements for the neutrinoless decay. Since ^{82}Se and ^{82}Kr are both considered to be intrinsically deformed [48], one may expect a recurrence of the fragmentation seen in ^{76}Ge [22]. However, in the present ^{82}Se case one only observes three relatively strong and a few rather weak GT transitions below 2 MeV, whereas in ^{76}Ge [22] there are in excess of 20 almost equally strong transitions distributed over the same excitation region. Above 2 MeV excitation energy though, the GT distributions of the two nuclei are qualitatively similar. Here the tails of the GTR extend into the low-energy region and give rise to many 1^+ states near the Fermi surface in both cases. Apparently, the extra two protons in the $(p_{3/2}p_{1/2}f_{5/2})$ and the extra four neutrons in the $(g_{9/2})$ configurations on top of ^{76}Ge, cause some stiffening of the nuclear shape and a concentration of GT strength in a few states near the Fermi surface. This trend seems to continue even beyond the $(Z = 40, N = 50)$ closed (sub)shells, like, e.g., for ^{96}Zr or ^{100}Mo, where almost all the low-energy GT strength relevant for $\beta\beta$ decay resides in a single state, which is the ^{96}Nb(694 keV) state for the ^{96}Zr case and the ^{100}Tc(g.s.) for the ^{100}Mo case [24,25]. At the same time the tails of the GTRs are pushed up in energy, and the GTRs themselves narrow around their central values near 13–15 MeV. Of course, a high-resolution charge-exchange reaction in the GT$^+$ direction on the daughter nucleus ^{82}Kr would be most desirable in order to understand in more detail the connection between deformation, resp. shape degrees of freedom and the $\beta\beta$-decay nuclear matrix elements.

TABLE IV. Solar neutrino capture rates on ^{82}Se as a function of excitation energy in ^{82}Br calculated from the B(GT) values listed in Tables II and III. Above $E_x = 2.5$ MeV the rates are evaluated for ± 0.25 MeV energy bins. The neutron separation energy is 7.592 MeV. The quoted error on the total SNU value is almost entirely determined by the uncertainty of the B(GT) value for the 75 keV state in ^{82}Br, which is of order 9%.

E_x	SNU	E_x	SNU	E_x	SNU	E_x	SNU
0.075	645.0	1.766	0.134	2.351	0.215	5.25	1.915
0.421	3.903	1.958	0.115	2.498	0.166	5.75	1.708
0.848	0.031	2.087	1.649	2.75	1.056	6.25	1.094
1.142	0.147	2.136	0.284	3.25	1.645	6.75	0.844
1.233	0.246	2.213	0.544	3.75	1.406	7.296	0.766
1.378	0.096	2.272	0.251	4.25	2.391	–	–
1.484	0.476	2.317	0.072	4.75	1.758		$\sum$668(±60)

D. Implications for solar neutrino detection

The low excitation energy of the first $J^\pi = 1^+$ state at 75 keV in ^{82}Br and the rather small ^{82}Se–^{82}Br mass difference of 96.6 keV [30] makes ^{82}Se a potentially attractive material for rather accurate solar neutrino measurements. A relatively large neutrino response can be expected, because the ^{82}Se(ν_e,e^-)^{82}Br*(75 keV) reaction cuts into a significant part of the pp-neutrino spectrum, which itself extends to $E_{\max} = 423.4$ keV [54]. In addition to this, ^{82}Br decays relatively quickly to ^{82}Kr ($T_{1/2} = 35.3$ h) via β-delayed γ-ray emission, which enables one to observe short-term solar neutrino-flux deviations, although likely not in real time. Techniques and details as well as real-time studies for other systems with similar properties are for instance described in Refs. [12,55,56].

Table IV lists the solar neutrino capture rates in a nonoscillation scenario as a function of the excitation energy in ^{82}Br using the B(GT) values given in Tables II and III. The rates for the individual components of the solar neutrino spectrum are presented in Table V. The calculations were carried out following the prescriptions given in Ref. [57] and using the solar neutrino fluxes from Ref. [51], where, except for the pp flux, which was constrained by the solar luminosity, these fluxes were determined from measurements by the Borexino, SNO, GALLEX/GNO/SAGE, and Super-Kamiokande experiments.

The total neutrino capture rate on ^{82}Se up to the neutron emission threshold at 7.592 MeV in ^{82}Br amounts to 668 SNU. The cumulative rates, which are shown in Fig. 7, indicate that about 97% of the captured solar neutrinos lead to the 1^+ state of ^{82}Br at 75 keV. This is a consequence of its relatively large B(GT) value and its sensitivity to a large part of the pp-neutrino spectrum. In fact, the pp neutrinos already account for 459 SNU.

The sudden increase of the SNU value at 421 keV excitation seen in Fig. 7 is a result of neutrinos from the ^{7}Be $\rightarrow$ ^{7}Li(g.s.) decay, which constitute the second largest component of the solar flux. This increase is made by the 421 keV, 1^+ state in ^{82}Br, which appears as a rather weak transition in the (^{3}He ,t) spectrum (cf. Fig. 2). The state captures ^{7}Be(g.s.) neutrinos,

TABLE V. Column one: solar neutrino components. Column two: cross sections calculated for B(GT) values reported here, assuming an oscillation-free neutrino spectrum. Column three: evaluated solar fluxes from the best fit to all solar neutrino experiments [51], where, except for the *pp* flux, which was constrained by the solar luminosity, the fluxes were determined from measurements of neutrinos by the Borexino, SNO, and Super-Kamiokande experiments. Column four: neutrino capture rates. The *hep* contribution of 0.15 SNU is obtained using the upper limit flux estimate of the SNO collaboration [52]. The uncertainties are evaluated from the solar flux uncertainties (column three), which are quoted in Ref. [51]. The ^{13}N, ^{15}O, and ^{17}F capture rates are combined into a single entry, where the 3σ upper limit for the summed fluxes quoted in Ref. [51] (i.e., 6.8×10^8 cm^{-2} s^{-1}) has been converted to a 1σ value with a 100% uncertainty. The fraction of each component is then taken from the BS05(OP) entries quoted in Ref. [53].

solar comp'nt	cross section [10^{-46} cm^2]	solar flux [cm^{-2} sec^{-1}]	capture rate [SNU]
pp	76.2	$6.02^{(1)}_{(6)} \times 10^{10}$	459(4)
pep	775	$1.63(34) \times 10^8$	12.7(26)
hep	126×10^3	$1.2(12) \times 10^4$	0.15(15)
^{7}Be(g.s.)	350	$4.48(24) \times 10^9$	156.5(84)
^{7}Be(477)	117	$0.51(2) \times 10^9$	6.0(2)
^{8}B	470×10^2	$5.39(16) \times 10^6$	25.3(8)
^{13}N	277	1.27×10^8	
^{15}O	464	0.97×10^8	8(8)
^{17}F	462	2.43×10^6	
			$\sum = 668 \pm 12$

but it lies outside the reach of *pp* and ^{7}Be(477) neutrinos. In comparison, the strong GT transition to the 2087 keV state has only a minor effect on the total SNU value since it can only be reached by the *hep* and ^{8}B neutrinos.

In Table IV we have quoted an uncertainty only for the total SNU value, since its error is almost entirely determined by the uncertainty of the B(GT) value for the 75 keV state in ^{82}Br, which is of order 9%. This value enters as a systematic uncertainty into the final value, whereas uncertainties of the rates calculations from the solar fluxes (Table V) can be treated as being of statistical nature. The final solar neutrino capture rate then comes to

$$R_\odot = 668 \pm 12(\text{sol}) \pm 60(\text{GT})\text{SNU}, \quad (7)$$

where the first error is due to the solar model and the second due to the rather conservatively calculated uncertainty of the B(GT) strength.

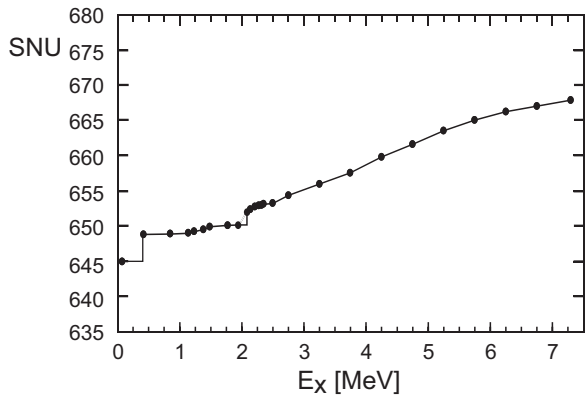

FIG. 7. Cumulative SNU values as a function of excitation energy in ^{82}Br.

IV. CONCLUSION

We have presented high-resolution (^{3}He,t) charge-exchange data on the $\beta\beta$ decay nucleus ^{82}Se. The data were taken at an incident energy of 420 MeV with an energy resolution of 38 keV. Angular distributions were measured, and B(GT) values were extracted for a multitude of states below 6 MeV excitation energy.

We have compared the present measurement on ^{82}Se with previous ones on systems close to the mass $A = 82$, which are ^{76}Ge on the lower mass side, and ^{96}Zr and ^{100}Mo on the higher mass side. We find that the (^{3}He,t) reaction on ^{82}Se shows properties, which are characteristic of both, the lighter and heavier systems. For instance, the pronounced fragmentation of B(GT) strength above 2 MeV is similar to what is overall observed for ^{76}Ge, whereas a concentration of B(GT) transition strength in a few low-lying states below 2 MeV is reminiscent of ^{96}Zr and ^{100}Mo. We have indicated that deformation and/or soft nuclear surfaces are the driving parameters for the GT fragmentation, which impact on the size of the nuclear matrix elements for $\beta\beta$ decay.

Apart from being a candidate for the neutrinoless $\beta\beta$-decay observation, we find that ^{82}Se could be of interest for the detection of solar neutrinos, in particular of those from the *pp* reaction. Based on the extracted B(GT) values we have calculated the SNU values for the detection of solar neutrinos to 668 SNU, of which *pp* neutrinos already contribute 459 SNU.

At the time of submission of this article, a new calculation for the solar neutrino fluxes based on a global analysis of neutrino data came to our attention [58]. The fluxes do not differ much from those appearing in Table V, except for the neutrinos from the CNO cycle. These new fluxes change the calculated SNU value quoted in Eq. (7) to $688 \pm 52(\text{sol}) \pm 61(\text{GT})$SNU. The increased error on the the solar model part is due to an increased uncertainty of the contribution from the CNO cycle.

ACKNOWLEDGMENTS

We thank the RCNP accelerator staff for their fine technical support during the course of the experiment. The generous financial support from the Directorate of RCNP is gratefully acknowledged. This work was supported by the Deutsche Forschungsgemeinschaft (DFG) under grant no. FR 601/3-1. M.A. acknowledges the financial support from Al-Nahrain University/Ministry of Higher Education and Scientific Research of Iraq. Y.F. and A.T. were partly supported by MEXT, Japan under Grant No. 22540310.

[1] D. L. Lincoln, J. D. Holt, G. Bollen, M. Brodeur, S. Bustabad, J. Engel, S. J. Novario, M. Redshaw, R. Ringle, and S. Schwarz, Phys. Rev. Lett. **110**, 012501 (2013).

[2] R. Arnold, C. Augier, J. Baker, A. Barabash, G. Broudin, V. Brudanin, A. J. Caffrey, E. Caurier, V. Egorov, K. Errahmane *et al.*, Phys. Rev. Lett. **95**, 182302 (2005).

[3] A. S. Barabash, Nucl. Phys. A **935**, 52 (2015).

[4] A. S. Barabash and V. B. Brudanin, Phys. At. Nucl. **74**, 312 (2011).

[5] J. W. Beeman, F. Bellini, L. Cardani, N. Casali, I. Dafinei, S. D. Domizio, F. Ferroni, L. Gironi, A. Giuliani, S. Nagorny *et al.*, J. Inst. **8**, P05021 (2013).

[6] J. W. Beeman, F. Bellini, P. Benetti, L. Cardani, N. Casali, D. Chiesa, M. Clemenza, I. Dafinei, S. D. Domizio, F. Ferroni *et al.*, Eur. Phys. J. C **75**, 591 (2015).

[7] W. Hampel, G. Heusser, J. Kiko, T. Kirsten, M. Laubenstein, E. Pernicka, W. Rau, U. Rönn, C. Schlosser, M. Wójcik *et al.*, Phys. Lett. B **420**, 114 (1998).

[8] F. Kaether, W. Hampel, G. Heusser, J. Kiko, and T. Kirsten, Phys. Lett. B **685**, 47 (2010).

[9] J. N. Abdurashitov, V. N. Gavrin, S. V. Girin, V. V. Gorbachev, T. V. Ibragimova, A. V. Kalikhov, N. G. Khairnasov, T. V. Knodel, V. N. Kornoukhov, I. N. Mirmov *et al.*, Phys. Rev. C **59**, 2246 (1999).

[10] J. N. Abdurashitov, V. N. Gavrin, S. V. Girin, V. V. Gorbachev, P. P. Gurkina, T. V. Ibragimova, A. V. Kalikhov, N. G. Khairnasov, T. V. Knodel, V. A. Matveev *et al.*, Phys. Rev. C **73**, 045805 (2006).

[11] J. N. Abdurashitov, V. N. Gavrin, V. V. Gorbachev, P. P. Gurkina, T. V. Ibragimova, A. V. Kalikhov, N. G. Khairnasov, T. V. Knodel, I. N. Mirmov, A. A. Shikhin *et al.*, Phys. Rev. C **80**, 015807 (2009).

[12] H. Ejiri, J. Engel, R. Hazama, P. Krastev, N. Kudomi, and R. G. H. Robertson, Phys. Rev. Lett. **85**, 2917 (2000).

[13] R. Madey, B. S. Flanders, B. D. Anderson, A. R. Baldwin, J. W. Watson, Sam M. Austin, C. C. Foster, H. V. Klapdor, and K. Grotz, Phys. Rev. C **40**, 540 (1989).

[14] W. Lin, O. Manuel, G. Cumming, D. Krstic, and R. Thorpe, Nucl. Phys. A **481**, 477 (1988).

[15] D. Frekers, P. Puppe, J. H. Thies, and H. Ejiri, Nucl. Phys. A **916**, 219 (2013).

[16] W. G. Love and M. A. Franey, Phys. Rev. C **24**, 1073 (1981).

[17] W. G. Love, in *Spin Excitations in Nuclei*, edited by F. Petrovich, G. E. Brown, G. T. Garvey, C. D. Goodman, R. A. Lindgren, and W. G. Love (Plenum Press, New York, London, 1982), pp. 205–232.

[18] M. A. Franey and W. G. Love, Phys. Rev. C **31**, 488 (1985).

[19] W. G. Love, A. Klein, M. A. Franey, and K. Nakayama, Can. J. Phys. **65**, 536 (1987).

[20] K. Nakayama and W. G. Love, Phys. Rev. C **38**, 51 (1988).

[21] E.-W. Grewe, D. Frekers, S. Rakers, T. Adachi, C. Bäumer, N. T. Botha, H. Dohmann, H. Fujita, Y. Fujita, K. Hatanaka *et al.*, Phys. Rev. C **76**, 054307 (2007).

[22] J. H. Thies, D. Frekers, T. Adachi, M. Dozono, H. Ejiri, H. Fujita, Y. Fujita, M. Fujiwara, E.-W. Grewe, K. Hatanaka *et al.*, Phys. Rev. C **86**, 014304 (2012).

[23] P. Puppe, D. Frekers, T. Adachi, H. Akimune, N. Aoi, B. Bilgier, H. Ejiri, H. Fujita, Y. Fujita, M. Fujiwara *et al.*, Phys. Rev. C **84**, 051305(R) (2011).

[24] J. H. Thies, T. Adachi, M. Dozono, H. Ejiri, D. Frekers, H. Fujita, Y. Fujita, M. Fujiwara, E.-W. Grewe, K. Hatanaka *et al.*, Phys. Rev. C **86**, 044309 (2012).

[25] J. H. Thies, P. Puppe, T. Adachi, M. Dozono, H. Ejiri, D. Frekers, H. Fujita, Y. Fujita, M. Fujiwara, E.-W. Grewe *et al.*, Phys. Rev. C **86**, 054323 (2012).

[26] P. Puppe, A. Lennarz, T. Adachi, H. Akimune, H. Ejiri, D. Frekers, H. Fujita, Y. Fujita, M. Fujiwara, E. Ganioğlu *et al.*, Phys. Rev. C **86**, 044603 (2012).

[27] D. Frekers, H. Ejiri, H. Akimune, T. Adachi, B. Bilgier, B. A. Brown, B. T. Cleveland, H. Fujita, Y. Fujita, M. Fujiwara *et al.*, Phys. Lett. B **706**, 134 (2011).

[28] D. Frekers, T. Adachi, H. Akimune, M. Alanssari, B. A. Brown, B. T. Cleveland, H. Ejiri, H. Fujita, Y. Fujita, M. Fujiwara *et al.*, Phys. Rev. C **91**, 034608 (2015).

[29] H. Ejiri, Phys. Rep. **338**, 265 (2000).

[30] G. Audi, M. Wang, A. H. Wapstra, F. G. Kondev, M. MacCormick, X. Xu, and B. Pfeiffer, Chin. Phys. C **36**, 1287 (2012).

[31] National Nuclear Data Center, Brookhaven National Laboratory (2014), http://www.nndc.bnl.gov.

[32] M. Fujiwara, H. Akimune, I. Daito, H. Fujimura, Y. Fujita, K. Hatanaka, H. Ikegami, I. Katayama, K. Nagayama, N. Matsuoka *et al.*, Nucl. Instrum. Methods Phys. Res. A **422**, 484 (1999).

[33] T. Wakasa, K. Hatanaka, Y. Fujita, G. P. A. Berg, H. Fujimura, H. Fujita, M. Itoh, J. Kamiya, T. Kawabata, K. Nagayama *et al.*, Nucl. Instrum. Methods Phys. Res. A **482**, 79 (2002).

[34] Y. Fujita, K. Hatanaka, G. P. A. Berg, K. Hosono, N. Matsuoka, S. Morinobu, T. Noro, M. Sato, K. Tamura, and H. Ueno, Nucl. Instrum. Methods Phys. Res. B **126**, 274 (1997).

[35] H. Fujita, G. P. A. Berg, Y. Fujita, K. Hatanaka, T. Noro, E. J. Stephenson, C. C. Foster, H. Sakaguchi, M. Itoh, T. Taki *et al.*, Nucl. Instrum. Methods Phys. Res. A **469**, 55 (2001).

[36] H. Fujita, Y. Fujita, G. P. A. Berg, A. D. Bacher, C. C. Foster, K. Hara, K. Hatanaka, T. Kawabata, T. Noro, H. Sakaguchi *et al.*, Nucl. Instrum. Methods Phys. Res. A **484**, 17 (2002).

[37] T. Noro, M. Fujiwara, O. Kamigaito, S. Hirata, Y. Fujita, A. Yamagoshi, T. Takahashi, H. Akimune, Y. Sakemi, M. Yosoi *et al.*, RCNP Annual Report (1991), p. 177.

[38] J. F. Ziegler (2011), http://www.srim.org.

[39] J. Cookand J. A. Carr, computer program FOLD, Florida State University, unpublished (1988), based on F. Petrovich and D. Stanley, Nucl. Phys. A **275**, 487 (1977),, modified as described in J. Cook, K. W. Kemper, P. V. Drumm, L. K. Fifield, M. A. C. Hotchkis, T. R. Ophel, and C. L. Woods, Phys. Rev. C **30**, 1538 (1984); and R. G. T. Zegers, S. Fracasso and G. Colò, NSCL, Michigan State University, unpublished (2006).

[40] J. Kamiya, K. Hatanaka, T. Adachi, K. Fujita, K. Hara, T. Kawabata, T. Noro, H. Sakaguchi, N. Sakamoto, Y. Sakemi *et al.*, Phys. Rev. C **67**, 064612 (2003).

[41] S. Y. van der Werf, S. Brandenburg, P. Grasdijk, W. A. Sterrenburg, M. N. Harakeh, M. B. Greenfield, B. A. Brown, and M. Fujiwara, Nucl. Phys. A **496**, 305 (1989).

[42] M. A. Hofstee, S. Y. van der Werf, A. M. van den Berg, N. Blasi, J. A. Bordewijk, W. T. A. Borghols, R. De Leo, G. T. Emery, S. Fortier, S. Galès *et al.*, Nucl. Phys. A **588**, 729 (1995).

[43] G. Perdikakis, R. G. T. Zegers, Sam M. Austin, D. Bazin, C. Caesar, J. M. Deaven, A. Gade, D. Galaviz, G. F. Grinyer, C. J. Guess *et al.*, Phys. Rev. C **83**, 054614 (2011).

[44] M. Ericson, T. Ericson, and P. Vogel, Phys. Lett. B **328**, 259 (1994).
[45] E. Caurier, F. Nowacki, A. Poves, and J. Retamosa, Nucl. Phys. A **654**, 973c (1999).
[46] J. Suhonen and O. Civitarese, Phys. Rep. **300**, 123 (1998).
[47] P. Sarriguren, E. Moya de Guerra, L. Pacearescu, A. Faessler, F. Šimkovic, and A. A. Raduta, Phys. Rev. C **67**, 044313 (2003).
[48] R. Álvarez-Rodríguez, P. Sarriguren, E. Moya de Guerra, L. Pacearescu, A. Faessler, and F. Šimkovic, Phys. Rev. C **70**, 064309 (2004).
[49] T. R. Rodríguez and G. Martínez-Pinedo, Phys. Rev. Lett. **105**, 252503 (2010).
[50] T. R. Rodríguez and G. Martínez-Pinedo, Progr. Part. Nucl. Phys. **66**, 436 (2011).
[51] A. Ianni, Phys. Dark Univ. **4**, 44 (2014).
[52] B. Aharmim, S. N. Ahmed, A. E. Anthony, E. W. Beier, A. Bellerive, M. Bergevin, S. D. Biller, M. G. Boulay, Y. D. Chan, M. Chen *et al.*, Astrophys. J. **653**, 1545 (2006).
[53] J. N. Bahcall, A. M. Serenelli, and S. Basu, Astrophys. J. Lett. **621**, L85 (2005).
[54] J. N. Bahcall, Phys. Rev. C **56**, 3391 (1997).
[55] H. Ejiri, J. Phys. Soc. Jpn. **74**, 2101 (2005).
[56] K. Zuber, Phys. Lett. B **571**, 148 (2003).
[57] H. Ejiri and S. R. Elliott, Phys. Rev. C **89**, 055501 (2014).
[58] J. Bergström, M. C. Gonzalez-Garcia, M. Maltoni, C. Peña-Garay, A. M. Serenelli, and N. Song, JHEP 03 (2016) 132.